# *Rapid Non-Destructive Detection Of Sub-Surface Cu in Silicon-On-Insulator Wafers by Optical Second Harmonic Generation*

## Advanced Metrology, Defect Inspection and Reduction

*V. Koldyaev, M. C. Kryger and J. P. Changala*
*Research and Development*
*Femtometrix, Inc.*
Santa Ana, California, USA
info@femtometrix.com

*M. L. Alles, D. M. Fleetwood, R. D. Schrimpf, N. Tolk*
*Dept. of EECS, School of Engineering*
*Vanderbilt University*
Nashville, Tennessee, USA
michael.alles@vanderbilt.edu

**Abstract --- Time dependent second harmonic optical signals were measured across silicon-on-insulator (SOI) wafer coupons contaminated by Cu-63 ion implanted into the buried oxide (BOX) and near the SOI/BOX and BOX/Bulk interfaces. Average signals after 1 second of exposure for all spatial points were compared between wafers and used to differentiate contamination levels post ion-implantation.**

**Keywords - AM: Advanced Metrology, DI: Defect Inspection and Reduction.**

## INTRODUCTION

Optical second harmonic generation (SHG) is a nondestructive, contactless, characterization method applicable to surfaces, interfaces and thin-films (Fig. 1) [1]. Unstrained Si films possess inversion symmetry, forbidding SHG within the layers, resulting in sensitivity primarily at surfaces, interfaces and in regions where electric fields break inversion symmetry.

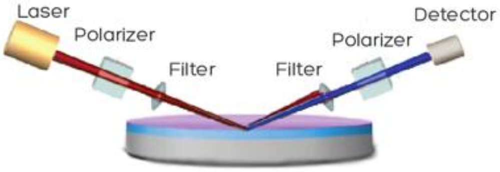

Figure 1: SHG on SOI wafer overview diagram.

Current tools used for SOI wafer characterization include methods to measure layer thickness and surface morphology; tools to analyze contamination on the surface, nondestructively, or below the surface, destructively; and electrical characterization techniques requiring invasive contacts. SHG satisfies the need for a nondestructive, noninvasive technique to characterize and map the properties of SOI interfaces across the wafer surface.

Optical SHG has been demonstrated in SOI materials [2-4] with the signal showing sensitivity to contamination [5], micro-roughness [6] and radiation induced defects [7]. SHG can be used to determine SOI band offsets [8] while bias dependent SHG signals have been shown to correlate with current-voltage plots [9].

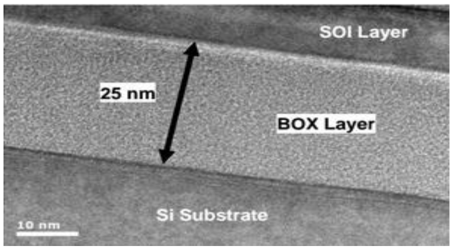

Figure 2: FD-SOI wafer cross section. [10]

Here, the time dependent SHG signal was measured without an applied bias. SHG signals were used to differentiate SOI wafers with varying doses of ion implanted Cu-63 in the BOX region between the BOX/Bulk and SOI/BOX interfaces (Figs. 2-4).

## II. PROCEDURE

Five 25x25mm coupons were cleaved from a single 12/25 nm SOI/BOX SOI wafer (Fig. 3), and four were ion implanted with Cu-63 at a tilt angle of 5 degrees and an energy of 30 keV. The calculations for placement of the Cu-63 at the BOX/Bulk and SOI/BOX interfaces were made using SRIM (Fig. 4). The fifth (control) sample was not implanted.

The top oxide of the wafer coupons was native, and no treatment was applied to the wafer before or after implantation. Measurements were carried out on the samples described above by irradiating the samples at 45° incident angle with p-polarized ~85 fs optical pulses (350 mW average power, 40 MHz repetition rate, wavelength $\lambda = 815$ nm) from a mode locked ultrashort pulse laser focused to a $w_0 \approx 50\ \mu$m radius spot on the surface of the sample. The p-polarized SH signal was spectrally filtered from the reflected fundamental beam and measured with an integrated photomultiplier element and photon counter as a function of time and discrete X-Y coordinates. All coupons were measured within 19 hours post-implantation. All SHG measurements were performed over a 10x10 rectilinear grid of spots with 1 mm spacing resulting in 121 data points on each coupon.

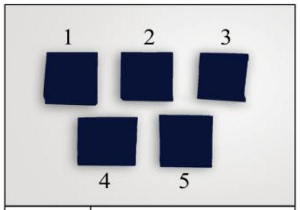

| Coupon | Implanted Dose |
|---|---|
| 1 | 5E9 Cu-63 atoms/cm² |
| 2 | 1E10 Cu-63 atoms/cm² |
| 3 | 1E11 Cu-63 atoms/cm² |
| 4 | 1E12 Cu-63 atoms/cm² |
| 5 | Control |

Figure 3: All 5 wafer coupons tested.

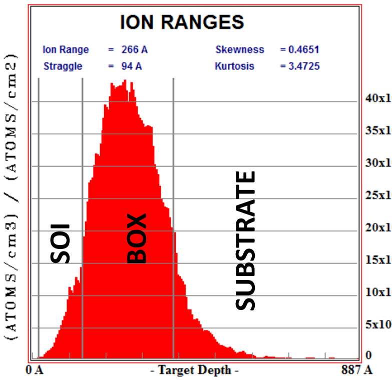

Figure 4: SRIM calculations for ion implantation doses.

## III. Results and Discussion

The scans indicate that SHG signal is directly proportional to the logarithm of the implanted Cu dose. Figure 5 shows the relationship between spatially averaged SHG signal during the first second of exposure time and implantation dose for the first scans done within 19 hours of ion implantation. The SHG signal is proportional to the logarithm of the implantation dose. The control sample is assigned an implantation dose of $10^9$ at/cm$^2$ in all relevant figures for comparison purposes.

Previous work has suggested that concentrations of copper above copper's solubility level in c-Si at room temperature precipitate with a time constant of $\tau_{precip}$ = 15 hours to deep traps and extended defects in the bulk as heterogeneous precipitation nucleation centers [11-14]. We suggest that a small leftover dose of copper from ion implantation is gettered initially at deep interfacial traps at the SOI/BOX and BOX/Bulk heterojunctions, which causes the initial proportional relationship between the SHG signal and implantation dose for the tests performed within t < 19 hours post ion implantation.

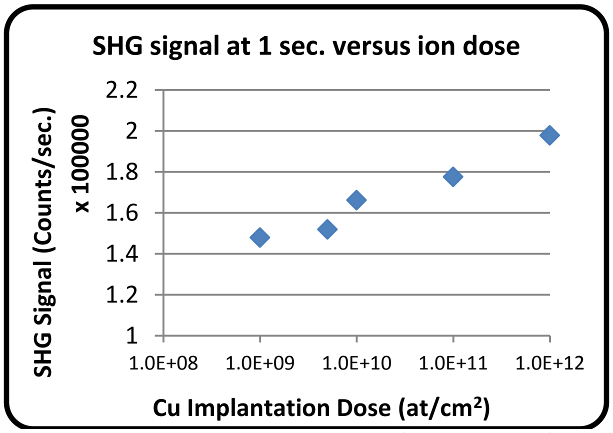

Figure 5: Spatially averaged SHG signals after one second of exposure from samples as a function of dose. The control wafer is assigned a dose of $10^9$ at/cm$^2$ for comparison purposes.

Tables 1 and 2 show estimated dose partitioning of copper in material layers and estimated volumetric Cu concentrations at the BOX/c-Si substrate interface, respectively. Dose partitioning was estimated by fitting a skewed Gaussian distribution to the SRIM data in Figure 4.

Estimated Partitioning of Ion Implanted Cu-63 at 5° Tilt and 30 keV

| *Parameter* | *% Cu Dose in Layer* |
|---|---|
| ***Native Oxide*** | 0.11 |
| ***Device SOI*** | 8.40 |
| ***BOX*** | 83.00 |
| ***Substrate (bulk c-Si)*** | 8.40 |

Estimated Volumetric Cu Concentrations at the BOX/c-Si Substrate Interface by Dose

| *Cu Dose (cm$^{-2}$)* | *Cu Concentration (cm$^{-3}$)* |
|---|---|
| $1.0 \times 10^{12}$ | $2.0 \times 10^{17}$ |
| $1.0 \times 10^{11}$ | $2.0 \times 10^{16}$ |
| $1.0 \times 10^{10}$ | $2.0 \times 10^{15}$ |
| $5.0 \times 10^{9}$ | $1.0 \times 10^{15}$ |

SHG is sensitive to the electric fields across interfaces, with the time-dependent electric field-induced second-harmonic (EFISH) signal from a single Si/SiO$_2$ interface described by Equation (1) [8],[9]:

$$I^{2\omega}(t) = |\chi^{(2)} + \chi^{(3)}E(t)|^2 (I^{\omega})^2 \tag{1}$$

$I^{\omega}$ and $I^{2\omega}$ are the fundamental and SHG signal intensities, respectively, while $\chi^{(2)}$ and $\chi^{(3)}$ are the second- and third-order susceptibilities, and E(t) is the electric field across the interface. The independent contribution of each interface to the measured SHG signal is demonstrated in Figure 6.

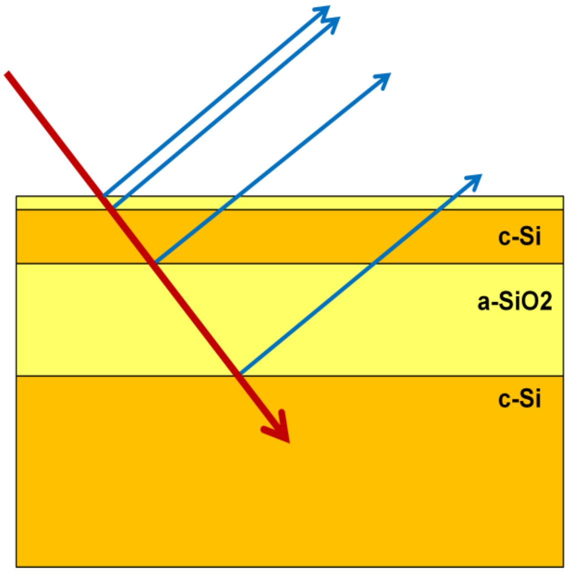

Figure 6: Contribution of each interface in SOI to measured SHG signal. Fundamental beam is NIR shown in red and SHG signal beams are UV shown in blue.

Critical parameters of Cu in c-Si and a-SiO$_2$

| *Parameter* | *c-Si* | *a-SiO$_2$* |
|---|---|---|
| ***Diffusivity (cm$^2$/s)*** | $1.3 \times 10^{-9}$ | $1.8 \times 10^{-22}$ |
| ***Diffusion length @ 8h (μm)*** | $6.05 \times 10^{1}$ | $2 \times 10^{-5}$ |

A statistical analysis was performed to determine the variation of the SHG signal across the tested coupons. The standard deviation of the signal at 1 second across each wafer coupon was found to be proportional to the ion implantation dose that wafer received, in absolute terms and as a fraction of the measured signal as well. Figure 7 reports the relationship between dose and signal variability measured as the standard deviation of SHG signal counts across the wafer coupon. If Cu remained dissolved in the c-Si, there would be no reason for systematic increase in the standard deviation of the signal for different doses. The statistically significant increase in the standard deviation for higher doses suggests that a strong Cu precipitation occurs, which causes Cu distribution across coupon to be more non-uniform. This agrees with the previous work concerning Cu precipitation in c-Si [12-14].

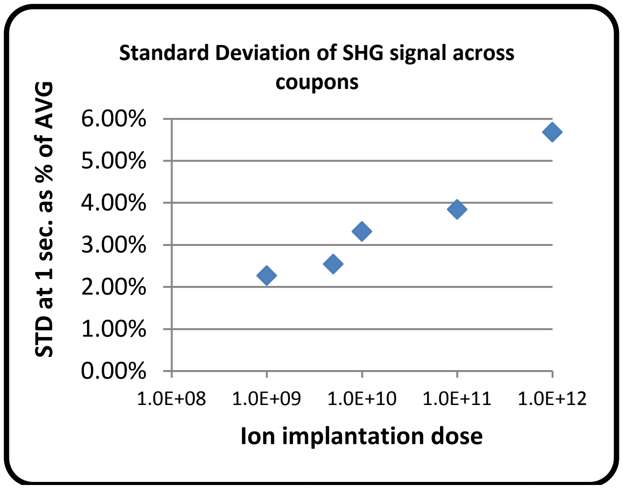

Figure 7: Standard deviation of SHG signal at 1 second, for all doses. Reported as % of SHG signal at 1 second. Control assigned a dose of 1E9 at/cm$^2$ for comparison purposes.

Regarding the physical mechanisms for changes in SHG due to the presence of Cu, there are several possibilities that can be investigated in future work:

(i) Cu atoms near the interfaces may cause mechanical stress by acting as dilation centers which can change second-order susceptibility, causing greater SHG response for higher Cu concentrations, (ii) Cu atoms reduce the carrier lifetimes of electron-hole pairs generated by the primary laser beam, which may increase the strength of the time-dependent electric field due to decreased screening of the built-in electric field, (iii) Higher Cu concentration in the BOX may provide more traps to capture electrons injected into the BOX by three-photon capture processes, creating an additional electric field that affects SHG, (iv) Cu ions implanted in SiO$_2$ may remain in charged states and change the electric field near the interfaces.

The Cu densities considered here are not high enough to create significant amounts of stress; thus, mechanism (i) is not likely the root cause. Mechanism (iv) is not likely the case because the change in the electric field is expected to be small. We conclude that mechanisms (ii) and (iii) are the most promising to evaluate in future work.

## IV. Summary

We have demonstrated SHG as a rapid, non-invasive and highly sensitive metrology technique to detect the presence of varying levels of buried copper contamination. Doses as low as $5 \times 10^{9}$ at/cm$^2$ have been detected, which is important for CMOS technology.

## V. Acknowledgments

Femtometrix, Inc. thanks Cutting Edge Ions LLC; Profs. S. Cristoloveanu, I. Ionica, A. Kaminski and G. Vitrant at IMEP Grenoble, as well as their lab members L. Pirro and V. Nguyen; and Drs. C. Mazuré and O. Kononchuk from Soitec.

## VI. REFERENCES

[1] T. Verbiest, K. Clays and V. Rodriguez, *Second-Order Nonlinear Optical Characterization Techniques, An Introduction*, CRC Press, Taylor & Francis Group, Boca Raton, FL, 2009.

[2] Y. Gu, T. Vu, and G. P. Li, "SOI material characterization using optical second harmonic generation," *Proc. IEEE Int. SOI Conf.*, pp. 94–95, Oct. 1994

[3] R. Pasternak et al. "Investigation of second-harmonic generation for SOI wafer metrology," *Proc. Int. Symp. Silicon-on-Insulator Technol. Devices XII*, pp. 87–92, May 2005.

[4] M. L. Alles et al. "Second Harmonic Generation for Noninvasive Metrology of Silicon-on-Insulator Wafers," *IEEE Trans. on Semicond. Manuf.*, vol. 20, pp 107-113, May 2007.

[5] M. L. Alles et al. "Experimental evaluation of second harmonic generation for non-invasive contamination detection in SOI wafers," *Proc. 17th Annu. IEEE/SEMI Advanced Semicond. Manuf. Conf.*, pp. 1–6, May 2006.

[6] J. L. Dadap et al. "Randomly oriented Angstrom-scale microroughness at the Si(100)/SiO interface probed by second harmonic generation," *Appl. Phys. Lett.*, vol. 64, no. 16, pp. 2139–2141, Apr. 1994.

[7] B. Jun et al. "Charge trapping in irradiated SOI wafers measured by second harmonic generation*," IEEE Trans. Nucl. Sci.*, vol. 51, pp. 3231–3237, Dec. 2004.

[8] Z. Marka et al. "Band Offsets Measured by Internal Photoemission-Induced Second-Harmonic Generation", *Phys. Rev. B*, vol. 67, 045302, pp. 1-5, Jan. 2003.

[9] B. Jun et al. "Characterization of multiple Si/$SiO_2$ interfaces in silicon-on-insulator materials via second-harmonic generation," *Appl. Phys. Lett*., vol. 85, no. 15, pp. 3095–3097, Oct. 2004.

[10] C. Pellisier. "Enabling substrate technology for a large volume fully depleted standard." *6th FD-SOI Workshop*, Feb. 2012.

[11] Y. Nishi and R. Doering. "Handbook of Semiconductor Manufacturing Technology." *CRC Press*. pp. 111, August, 2000.

[12] A. A. Istratov et al., "Interstitial copper-related center in n-type silicon," *Appl. Phys. Lett*., vol. 71, 2349 (1997).

[13] A. A. Istratov et al., "Effects of copper on diffusion length and lifetime of minority carriers in p-type silicon," *Appl. Phys. Lett*., vol. 71, 2121 (1997).

[14] M. Seibt et al., "Formation and properties of copper silicide precipitates in silicon," *Phys. Stat. Sol*., vol. 166, 171 (1998).